Realization of absolute negative refraction index by a photonic crystal using anisotropic dielectric material

Yuntuan Fang (方云团)[1] and Zhengbiao Ouyang (欧阳征标)[2,3,4]

[1] *Department of Physics, Zhenjiang Watercraft College, Zhenjiang 212003*

[2] *THz-Technology Research Center of Shenzhen University, Shenzhen 518060*

[3] *Shenzhen Key Laboratory of Micro-Nano-Photonic Information Technology, Shenzhen 518060*

[4] *College of Electronic Science and Technology of Shenzhen University, Shenzhen 518060*

Received September 4, 2007

A method to realize absolute negative refraction index −1 with a two-dimensional (2D) photonic crystal is presented by introducing dielectric anisotropy in the photonic crystal material. The band structures of E-polarization mode and H-polarization mode can be adjusted by changing the parameters of materials. Thus the two modes with different polarizations have the same negative refraction index −1 for the same frequency. The results are demonstrated by numerical simulation based on the finite-difference time-domain (FDTD) method.

OCIS codes: 250.0250, 160.4670, 260.1180, 110.2990.

Since the concept of the left-handed materials (LHMs) or negative refraction index materials (NRIMs) was proposed by Veselago in 1968, negative refraction has attracted great interest in the flat slab imaging[1−21], which can be realized through photonic crystals (PCs) or LHMs. For PCs, the equifrequency surface (EFS) of Bloch's modes can be properly designed, so that the group velocity (directed to the EFS normal) of a Bloch's mode excited by an incident wave may point to a negative-refraction direction[2]. Many researchers[2−9,16−21] verified that a point source on one side of a two-dimensional (2D) PC slab could generate a real point image on the opposite side. They also attempted to connect this phenomenon to the mechanism of superlensing. The superlensing effect can potentially overcome the diffraction limit inherent in conventional lenses. In these PC structures, there are two kinds of cases for negative refraction. The first is that the direction of the group velocity is anti-parallel to the wave vector $\vec{k}$ within the PC, thus an effective index of negative refraction n_{eff} can be defined (for simplicity, we call effective negative refraction index as negative refraction index)[2]. Another case is that the direction of the group velocity is not anti-parallel to the wave vector $\vec{k}$, and the negative refraction can be realized without employing a negative index material. In this case, a negative refraction index cannot be defined[3,4]. It is well known that the electromagnetic wave can be decomposed into the E- and H-polarization modes for a 2D structure. However, most of the studies on the negative refraction of 2D PCs focused on a certain polarized wave, i.e., the E-polarization mode or H-polarization mode. Ao *et al.*[22] created a photonic crystal beamsplitter using opposite refraction behavior for two different polarizations. As for whether a negative refraction index of a PC could exist for both polarized waves at the same frequency, Zhang[4] demonstrated that the complete negative refraction regions for all polarizations existed in some metallodielectric PC structures. However, a negative refraction index for both polarized waves has not been found yet. In this paper, we will demonstrate that a negative refraction index of $n_{\mathrm{eff}} = -1$ for both polarized waves at the same frequency can be realized by a 2D PC through introducing anisotropic dielectric material in the PC. We call it as absolute negative refraction index. The results indicate that negative refraction index for unpolarized light can be realized. This idea partly comes from Ref. [23], which introduced a method to obtain large absolute band gap in 2D anisotropic PCs.

To realize negative refraction, the three-dimensional (3D) PC band structures should be convex, and the constant-frequency contours are circle and larger than those of air, i.e., circles with radii ω/c[2,3,5]. Then, for one frequency with constant-frequency contour radius equal to that of air, the effective refraction index is −1. For a given PC structure, it is impossible that the photonic band structures are the same for the two polarization modes, then we cannot generally obtain absolute negative refraction index of −1. However, the positions of the photonic band can be adjusted by varying the refractive index contrasts for the E-polarization and H-polarization modes in a given PC[23]. In such a way, the frequencies corresponding to a negative refraction index of $n_{\mathrm{eff}} = -1$ for both modes can be adjusted to the same value, thus the absolute negative refraction index will be obtained. One way available is to fabricate PC from anisotropic dielectric material. And there are a lot of anisotropic crystals in nature, which are lossless and transparent in visible or infrared regime[23].

Here we first select a 2D PC made of triangular lattice of air holes in anisotropic medium tellurium (Te), which is a uniaxial crystal with ordinary dielectric constant $\varepsilon_{\mathrm{o}} = 23.04$ and extraordinary dielectric constant $\varepsilon_{\mathrm{e}} = 34.88$. The radius of air hole is $0.35a$, where a is the lattice constant. Different from Ref. [23], we choose the ordinary axis of the uniaxial crystal parallel to, and the extraordinary axis perpendicular to the extensional direction of air holes respectively. Therefore the electric field vector in the E-polarization mode is parallel to the ordinary axis, while perpendicular to the ordinary axis in the H-polarization mode. Maxwell equations for such anisotropic 2D photonic band structure are the same as those for the isotropic photonic band structures, except that the dielectric constants for the two modes are different. Then we can calculate the photonic band structures for two polarization modes using the plane-wave expansion method[24]. Figures 1(a) and (b) show the photonic band structures for the H-polarization and E-polarization modes, respectively. According to the negative refraction conditions[2,3,5] and the calculation results, the negative refraction could occur in the third band for the H-polarization mode and in the second band for the E-polarization mode. Figure 2 gives the constant-frequency contours of the third band for the H-polarization mode. The shapes of EFS are almost circular for higher frequencies, which means that the wave propagations of these frequencies are isotropic-like. For the isotropic frequency range, the effective refractive-index concept can be used for studying light propagation, and light refraction can be simply described by the Snell law[2]. This index is the phase index of refraction since it is defined by the phase velocity, $n_{\mathrm{p}} = k/k_0$, where k and k_0 are the wave vectors in the photonic crystal and in vacuum, respectively. Meanwhile, the direction of group velocity vector $\mathbf{v}_{\mathrm{g}} = \nabla_k \omega$ is the direction of the energy flow, which is normal to the EFS. Since the group velocity for the second band is negative due to the all-convex shape of the EFS, the directions of waves are inward from the circular EFS. To clearly describe it, the schematic wave-vector diagrams are shown in Fig. 3 for the wave propagation from air to the PC. The two

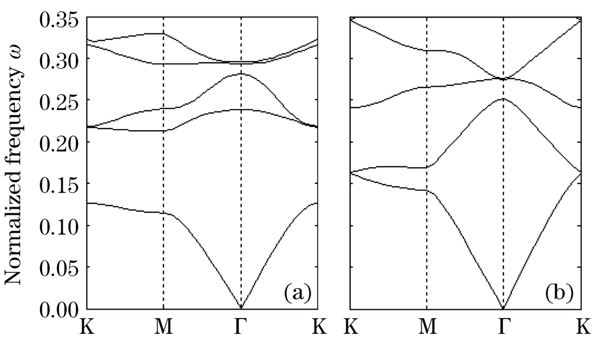

Fig. 1. Photonic band structures for (a) the H-polarization and (b) the E-polarization modes.

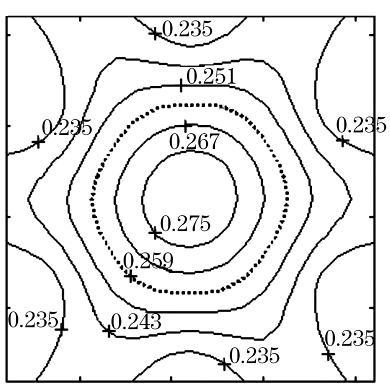

Fig. 2. Constant-frequency contours of the third band for the H-polarization mode.

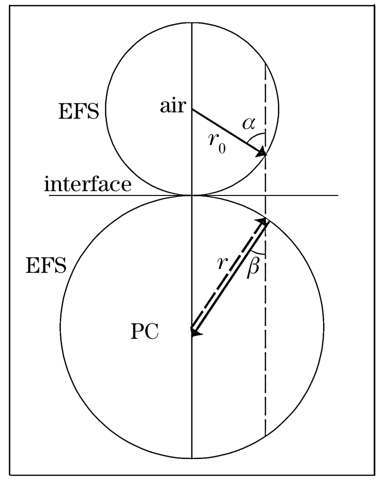

Fig. 3. Schematic wave-vector diagrams for the wave propagation from air to the PC.

solid arrows indicate two wave vectors from two different spaces, and the dash arrow refers to the group velocity vector in the PC[25]. Remember that the continuity of tangential components of the wave vector across the interface determines the **k** vector in the second material. Thus the effective negative refraction index for a certain frequency can be calculated by $n_{\mathrm{eff}} = -\frac{\sin\alpha}{\sin\beta} = -\frac{r}{r_0}$, where r_0 and r are the radii of two EFSs for the same frequency in air and the PC, respectively. The equal frequency contour obtained by crossing the second band with the equal frequency surface for $\omega = 0.259(2\pi c/a)$ (for simplicity, the unit $2\pi c/a$ of frequency is omitted in the following) is circular and convex, and thus has inward-pointing group velocity. This results in negative propagation angles for all incident angles. The propagations of the waves are therefore isotropic, and one can define an isotropic effective refraction index n_{eff} from the radius of the EFS using the Snell law[2]. For current frequency $\omega = 0.259$, the effective refractive index of the PC is near to -1 which is indicated by dotted line in Fig. 3.

Figure 4 plots the second band of the E-polarization mode (circle line) in Fig. 1(a). Clearly, the whole second band for the E-polarization mode is below the line of $\omega = 0.259$, thus absolute negative refraction index -1

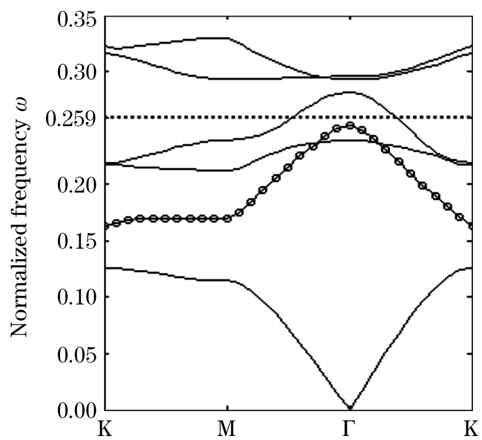

Fig. 4. Second band (circle line) for the E-polarization mode in the photonic band structures for the H-polarization mode.

cannot be obtained in this case. However, as the photonic band frequency is somewhat inversed with respect to the dielectric constant contrast of PC, we can raise the second band for the E-polarization mode by decreasing the value of ε_o. In order to observe the relation of the photonic band frequency and the value of ε_o, we only calculate the second band for the E-polarization mode for different values of ε_o.

Figure 5 plots the influence of ε_o on the band diagram, which verifies that the photonic band frequency increases with the decreasing of ε_o. By carefully decreasing the value of ε_o, we finally make the second band for the E-polarization mode (square line), the third band for the H-polarization mode (solid line) and the line of $\omega = 0.259$ (dot line) intersect approximately at two points, as indicated in Fig. 6. Here the value of ε_o is 16.3. In this case, we plot the constant-frequency contour in Fig. 7 (bold line) for $\omega = 0.259$ for the E-polarization mode in Fig. 2 again. As a result, the two constant-frequency contours for $\omega = 0.259$ almost close up in spite of a little difference. Now we can conclude that for $\omega = 0.259$, the negative refraction index for the E-polarization mode approximately equals to -1. Then for the same frequency we obtain the same negative refraction index -1 from the 2D anisotropic PC, i.e., absolute negative refraction index is nearly realized.

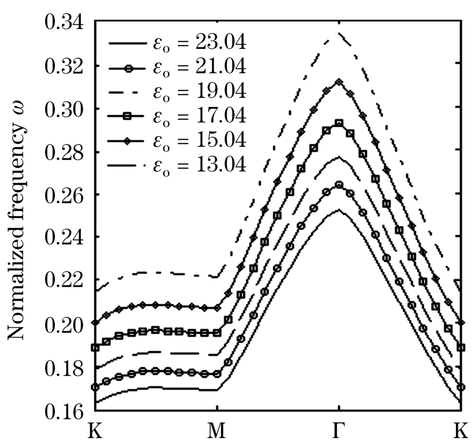

Fig. 5. Influence of ε_o on the band diagram at the second band for the E-polarization mode.

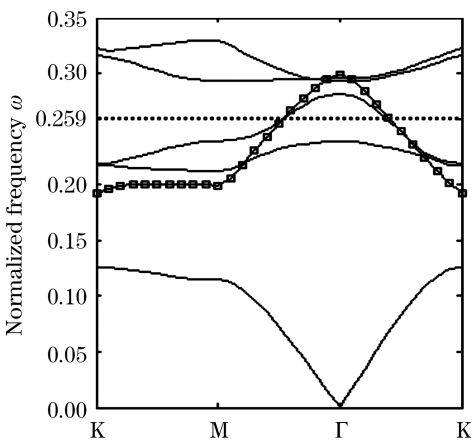

Fig. 6. Second band (square line) for the E-polarization mode with $\varepsilon_o = 16.03$ in the photonic band structures for the H-polarization mode.

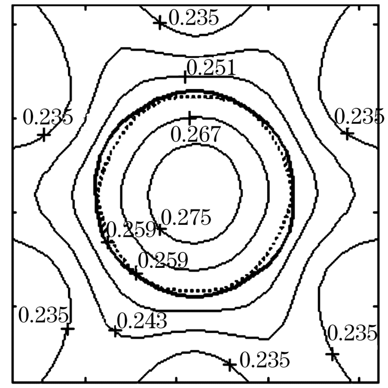

Fig. 7. Constant-frequency contour of $\omega = 0.259$ for the E-polarization mode (bold line) in the constant-frequency contours of the third band for the H-polarization mode.

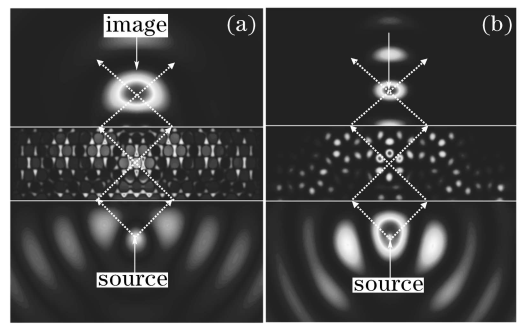

Fig. 8. Distributions of electric field intensity with a same source frequency $\omega = 0.259$ for (a) the H-polarization mode and (b) the E-polarization mode.

In order to verify the above results, we perform a numerical simulation based on the finite-difference time-domain (FDTD) method[26] adopting a perfectly matched layer (PML) boundary[27]. The FDTD method is a very powerful method to analyze electromagnetic problem due to its simplicity and accuracy. In our computation, the surface normal of the 2D PC is along the ΓM direction, and a point source with frequency $\omega = 0.259$ is placed at a distance $2a$ from one side of the 2D-PC slab with a width of $4a$. The source excites electromagnetic waves corresponding to two polarization modes. Figures 8(a) and (b) plot the magnetic field intensity for the H-polarization mode and the electric field intensity for the E-polarization mode in the computing space, respectively. Obviously, the light directions indicated by white arrows both basically obey the Snell law for $n_{\mathrm{eff}} = -1$. It should be noticed that the intensities around the center of the PC structure are the biggest in the whole PC structure (see Figs. 8(a) and (b)). The bright spots are just inner images which further demonstrate that the outer images result from negative refraction, not self-collimation effect. As a result, a single PC structure focuses a point source with the same frequency into point images on its opposite side for both polarization modes. We also find that the quality of image for the H-polarization mode is a little worse than that for the E-polarization mode, for the two EFSs do not absolutely superpose. In this case, absolute negative refraction index has been demonstrated, and the image of an unpolarized light source has been realized.

In conclusion, we bring forward a concept of absolute negative refraction index with PC. In order to realize it, we introduce dielectric anisotropy in the background medium of a 2D PC. Because nature offers large varieties of anisotropic material, our work opens up a scope for the application of negative refraction of PC.

This work was supported by the National Natural Science Foundation of China (No. 60471047), the Natural Science Foundation of Guangdong Province (No. 04011308), and the Shenzhen Bureau of Science and Technology. Y. Fang's e-mail address is fang_yt1965@sina.com.

References

1. V. G. Veselago, Sov. Phys. Uspekhi **10,** 509 (1968).
2. M. Notomi, Phys. Rev. B **62,** 10696 (2000).
3. C. Y. Luo, S. G. Johnson, J. D. Joannopoulos, and J. B. Pendry, Phys. Rev. B **65,** 201104 (2002).
4. X. Zhang, Phys. Rev. B **70,** 205102 (2004).
5. M. Qiu, L. Thylen, M. Swillo, and B. Jaskorzynska, IEEE J. Sel. Top. Quantum Electron. **9,** 106 (2003).
6. X. Zhang, Phys. Rev. B **71,** 165116 (2005).
7. X. Zhang, Phys. Rev. B **70,** 195110 (2004).
8. R. Moussa, S. Foteinopoulou, L. Zhang, G. Tuttle, K. Guven, E. Ozbay, and C. M. Soukoulis, Phys. Rev. B **71,** 085106 (2005).
9. C. Y. Luo, S. G. Johnson, J. D. Joannopoulos, and J. B. Pendry, Phys. Rev. B **68,** 045115 (2003).
10. Z.-Y. Li and L.-L. Lin, Phys. Rev. B **68,** 245110 (2003).
11. H.-T. Chien, H.-T. Tang, C.-H. Kuo, C.-C. Chen, and Z. Ye, Phys. Rev. B **70,** 113101 (2004).
12. S. He, Z. Ruan, L. Chen, and J. Shen, Phys. Rev. B **70,** 115113 (2004).
13. W. Jiang, R. T. Chen, and X. Lu, Phys. Rev. B **71,** 245115 (2005).
14. S. Foteinopoulou and C. M. Soukoulis, Phys. Rev. B **67,** 235107 (2003).
15. E. Cubukcu, K. Aydin, E. Ozbay, S. Foteinopoulou, and C. M. Soukoulis, Nature **423,** 604 (2003).
16. P. V. Parimi, W. T. Lu, P. Vodo, and S. Shridar, Nature **426,** 404 (2003).
17. Z. Ruan, M. Qiu, S. Xiao, S. He, and L. Thylén, Phys. Rev. B **71,** 045111 (2005).
18. Y. Fang, Y. Liu, and T. Shen, Chin. Opt. Lett. **4,** 230 (2006).
19. K. Guven, K. Aydin, K. B. Alici, C. M. Soukoulis, and E. Ozbay, Phys. Rev. B **70,** 205125 (2004).
20. X. Wang, Z. F. Ren, and K. Kempa, Opt. Express **12,** 2919 (2004).
21. X. Wang and K. Kempa, Phys. Rev. B **71,** 233101 (2005).
22. X. Y. Ao and S. L. He, Opt. Lett. **30,** 2152 (2005).
23. Z.-Y. Li, B.-Y. Gu, and G.-Z. Yang, Phys. Rev. Lett. **81,** 2574 (1998).
24. K. M. Ho, C. T. Chan, and C. M. Soukoulis, Phys. Rev. Lett. **65,** 3152 (1990).
25. Y.-T. Fang, Q. Zhou, and E. Y. B. Pun, Appl. Phys. B **86,** 587 (2006).
26. K. S. Yee, IEEE Trans. Antennas and Propagat. **14,** 302 (1966).
27. J. P. Berenger, J. Comput. Phys. **114,** 185 (1994).